Bioresource Technology 262 (2018) 184–193

Contents lists available at ScienceDirect

Bioresource Technology

journal homepage: www.elsevier.com/locate/biortech

Organic loading rate and hydraulic retention time shape distinct ecological networks of anaerobic digestion related microbiome

Rui Xu[a,b], Zhao-Hui Yang[a,b,*], Yue Zheng[c], Jian-Bo Liu[a,b], Wei-Ping Xiong[a,b], Yan-Ru Zhang[a,b], Yue Lu[a,b], Wen-Jing Xue[a,b], Chang-Zheng Fan[a,b]

[a] College of Environmental Science and Engineering, Hunan University, Changsha 410082, PR China
[b] Key Laboratory of Environmental Biology and Pollution Control (Hunan University), Ministry of Education, Changsha 410082, PR China
[c] Department of Chemical Engineering, University of Washington, Seattle, WA 98195, United States

ARTICLE INFO

Keywords:
Anaerobic digestion
Organic loading rate
Hydraulic retention time
Microbial diversity
Network analysis

ABSTRACT

Understanding of how anaerobic digestion (AD)-related microbiomes are constructed by operational parameters or their interactions within the biochemical process is limited. Using high-throughput sequencing and molecular ecological network analysis, this study shows the succession of AD-related microbiome hosting diverse members of the phylum *Actinobacteria*, *Bacteroidetes*, *Euryarchaeota*, and *Firmicutes*, which were affected by organic loading rate (OLR) and hydraulic retention time (HRT). OLR formed finer microbial network modules than HRT (12 *vs.* 6), suggesting the further subdivision of functional components. Biomarkers were also identified in OLR or HRT groups (e.g. the family *Actinomycetaceae*, *Methanosaetaceae* and *Aminiphilaceae*). The most pair-wise link between *Firmicutes* and biogas production indicates the keystone members based on network features can be considered as markers in the regulation of AD. A set of 40% species ("core microbiome") were similar across different digesters. Such noteworthy overlap of microbiomes indicates they are generalists in maintaining the ecological stability of digesters.

1. Introduction

In the past years the increased significance of the renewable energy (mainly methane) recovered from anaerobic digestion (AD) has attracted considerable interest in the application of this promising technology to wastewater, municipal waste sludge, urban organic waste or new co-digestion feedstocks (Dareioti and Kornaros, 2014; Fitamo et al., 2017; He et al., 2018; Wu et al., 2016; Xu et al., 2015). AD technology supports the energy balance in wastewater treatment plants which are energy consuming (Kundu et al., 2017). Previous studies reported the methane generation strongly correlate with many AD parameters. For example, organic loading rate (OLR), hydraulic retention time (HRT), pretreatment, temperature, pH, etc., have been confirmed to be associated directly with AD process (Gou et al., 2014; Kumar et al., 2016; Xu et al., 2018; Ziganshin et al., 2016). Our previous study also showed that reactor's stability and microbial metabolic activity is strongly affected by OLR and HRT (Xu et al., 2015). Despite the "black box" of AD is partially unraveled, however, as an important microbial process, there is still more to be understood the crucial correlations between microbial community structure and function for more efficient and predictable AD performance.

During the biochemical pathways of AD, critical intermediates are converted to methane *via* different microbial groups, including *Archaea* and *Bacteria* (Dareioti and Kornaros, 2014; Fitamo et al., 2017; Xu et al., 2018). Recent studies have used multiple advanced "-omics" technologies to profile the composition and variation of microbial community in AD process (Anantharaman et al., 2016; De Vrieze et al., 2018; Kundu et al., 2017; Qin et al., 2016; Xu et al., 2017). Former researchers found that the variations of function microbes largely depend on reactor design as well as many operational variables, such as temperature, OLR or HRT (Gou et al., 2014; Razaviarani and Buchanan, 2014; Xu et al., 2018; Ziganshin et al., 2016). In a previous survey across seven full-scale anaerobic digesters located in Europe, Riviere et al., identified the phylum *Chloroflexi*, *Betaproteobacteria*, *Bacteroidetes* and *Synergistetes* as the core members involve in AD of sludge (Rivière et al., 2009). This study also shows current knowledge on the dynamics between microbiomes and AD operation is still limited. Because the microbial communities across AD steps (including hydrolysis, acidogenesis, acetogenesis and methanogenesis) have been characterized to host a high abundance of microbial diversity. Most of them are detected at the low abundance (< 0.1%) of "rare biosphere" (Anantharaman et al., 2016; Lynch, 2015), little reliable information is known about

* Corresponding author at: College of Environmental Science and Engineering, Hunan University, Changsha 410082, PR China.
E-mail address: yzh@hnu.edu.cn (Z.-H. Yang).

https://doi.org/10.1016/j.biortech.2018.04.083
Received 29 March 2018; Received in revised form 19 April 2018; Accepted 20 April 2018
Available online 22 April 2018

how such complex microbial communities in AD system are structured, and how reactor parameters shape the inter-organism interactions (Kundu et al., 2017; Razaviarani and Buchanan, 2014). This restricts the understanding of microbial population and evolution, or which keystone species affect AD process. This study proposes an assumption about the "core microbiomes" that the species common to all or nearly all AD conditions, which is essential component for methane production or digesters stability. The minimal variation of "core microbiomes" should be detectable from different dataset. These fundamental populations can be considered as marker species that reflecting the conditions in AD digesters.

Furthermore, the previously operation taxonomic units (OTUs)-based investigation of AD-related microbiomes mainly focused on how individual member within each reactor is affected by different operational conditions (Wu et al., 2016). However, this approach can not reveal the complex interactions that occur in microbial communities. Because microbes cooperate within close metabolic interactions, providing each other with critical nutrients for their growth (De Vrieze et al., 2016; Deng et al., 2012; Edwards et al., 2015). For instance, the acetate that utilized by methanogenic *Archaea* for methane generation mainly come from the fermentative *Bacteria* (Wu et al., 2016); while an increase of ammonia concentration in AD digesters often caused a transition of methanogenic pathway from acetoclastic to hydrogenotrophic methanogenesis (De Vrieze et al., 2016). Thus, further studies are required to focus on the microbial cooperation at the overall community level, because it is expected to affect more to ecological functions than individual members (Ma et al., 2016; Wu et al., 2016). Nevertheless, it is a great challenge to identify the interactions within microbial community because their vast diversity and uncultivated status (Deng et al., 2012). Molecular ecological network analysis (MENA) provides a new approach towards deducing microbial interactions within the complicated communities, which has been successfully performed in various habitats, including soils, human gut and oceans (Faust and Raes, 2012; Wu et al., 2016). This analysis can identify the keystone species and their interactions with other taxa. It helps to understand how synergistic biochemical reactions of AD-related microbiomes are affected by the different operational parameters.

To address these questions, this study presents a detailed characterization of the AD-related microbiomes by high throughput sequencing (HTS) approach and network analysis by running three AD reactors under controlled conditions of OLR and HRT. The purpose is the extensive recognition of ecological roles of AD parameters to shape microbial majority. This was achieved by: (1) using HTS targeting microbial communities to cover different operational periods from three AD reactors. (2) comparing microbial distribution and dynamics under different OLR and HRT conditions. (3) correlating the variation of individual microbe within ecological network.

2. Materials and methods

2.1. Preparation of substrates and feedstock materials

The seed sludge (SS) and feedstock materials including municipal waste sludge (MWS), raw food waste (FW) with high a concentration of fat, oil and grease (FOG) were collected from several locations in China, as described in (Xu et al., 2015). The most commonly used substrates of MWS and FW for AD has been widely documented to enhance biogas production or nutrient balance (Kumar et al., 2016; Xu et al., 2015). FOG was separated from raw FW using a cement compressor and Soxhlet extraction method. The MWS and post-treated FW (considered as no FOG) were smashed into small particles using an electric food grinder (XTL-767, IFAVORITE) and mixed with a TS ratio of 1: 1. The mixture of MWS and post-treated FW was identified as "substrates" in the following parts. Materials used in this study was characterized in terms of common AD physico-chemical properties (see Supplementary data). The detail analytical methods and values are described in (Xu et al., 2015).

Table 1
Summary of experiment setups and OTU numbers in R1, R2 and R3.

Sample	Period	HRT (d)	Phylum (59)	OTUs shared ratio (detected OTUs' number)			
				Class (155)	Order (259)	Family (318)	Genus (645)
R1-1	I	20	76%	65%	60%	74%	44%
R1-18	I	20	75%	59%	51%	64%	33%
R1-30	I	20	75%	57%	49%	58%	30%
R1-40	II	20	76%	62%	53%	61%	35%
R1-57	II	20	71%	41%	35%	52%	25%
R1-72	III	20	64%	49%	43%	52%	29%
R1-85	III	20	69%	59%	52%	64%	40%
R1-91	IV	20	64%	52%	46%	57%	32%
R1-109	IV	20	69%	64%	54%	66%	40%
R1-120	IV	20	73%	57%	50%	64%	38%
R2-1	I	20	81%	70%	64%	75%	45%
R2-18	I	20	81%	63%	56%	69%	45%
R2-30	I	20	66%	53%	45%	58%	34%
R2-40	II	20	46%	43%	38%	56%	29%
R2-57	II	20	61%	48%	43%	62%	30%
R2-72	III	20	61%	55%	46%	63%	37%
R2-85	III	20	59%	46%	37%	56%	27%
R2-91	IV	20	64%	53%	44%	58%	31%
R2-109	IV	20	64%	55%	44%	59%	31%
R2-120	IV	20	63%	49%	41%	56%	28%
R3-1	I	15	80%	66%	58%	67%	39%
R3-18	I	15	85%	58%	51%	60%	31%
R3-30	I	15	68%	56%	47%	62%	36%
R3-40	II	15	61%	41%	36%	49%	27%
R3-57	II	15	59%	49%	47%	60%	37%
R3-72	III	15	58%	48%	41%	57%	34%
R3-85	III	15	63%	55%	47%	65%	39%
R3-91	IV	15	61%	54%	46%	58%	32%
R3-109	IV	15	64%	58%	51%	63%	35%
R3-120	IV	15	66%	55%	49%	62%	36%

2.2. AD experiment procedure

AD experiment was conducted in nine (R1, R2, R3 in triplicates) continuously stirred reactors (CSTR) with 2.0 L working volume over 120 days at a mesophilic condition. Each reactor was operated under different OLR and HRT conditions across 4 periods (Table 1). R1 was operated under invariable OLR ($3\,g\,VS\,L^{-1}\,d^{-1}$, only the substrates) and HRT (20 day) as the control. R2 received a gradient increasing OLR from 4.5 to $6.7\,g\,VS\,L^{-1}\,d^{-1}$ (performed by adding different FOG contents in co-digestion with the substrates) in 4 periods with a constant HRT = 20 day. R3 received the OLR as R2 but HRT = 15 day. Samples from each reactor were periodically collected for the routine chemical analysis, including biogas production, pH, chemical oxygen demand (COD), total solids (TS), volatile solids (VS), volatile fatty acids (VFA), alkalinity (ALK), total carbon (TC) and total nitrogen (TN), etc. Detailed information of the set-up and start-up of each reactors can be found in the previous work (Xu et al., 2015). Performance data of typical processes (such as the begin, mid-term and end of each period) used in this study are summarized in Supplementary data.

2.3. DNA extraction and high-throughput sequencing

For the HTS analysis, 90 samples from R1, R2 and R3 were collected on day 1, 18, 30, 40, 57, 72, 85, 91, 109, 120 to cover the whole digestion process. All samples were: (1) stabilized using 50% (v/v) alcohol, (2) flushed three times with 0.1 M Na_3PO_4 (pH = 8), (3) vortexed at maximum speed for 5 min in the sodium dodecyl sulfonate reagent to thoroughly lyse, (4) genomic DNA was extracted from ~1.0 g of each in triplicates according to the instructions of FastDNA

SPIN Kit for Soil, (5) the extracted DNA was determined for concentrations and quality using a NanoDrop spectrophotometer, (5) all qualified DNA were dissolved in Tris buffer (~150 ng uL^{-1}) for the downstream polymerase chain reaction (PCR).

Bar-coded primer pair were selected to target the variation fragment of 16S rRNA genes using 515F/907R (Kuczynski et al., 2011). PCR amplification was conducted with a final volume of 20 μL following previously study (Xu et al., 2018). The amplification cycles followed with an initial denaturation at 98 °C for 1 min, 30 cycles of denaturation at 98 °C for 10 s, 50 °C annealing for 30 s and 72 °C for 30 s extension. A final extension at 72 °C for 5 min was included before holding at 4 °C. PCR raw products were purified using the GENECLEAN Turbo Kit (MP Bio, USA). The qualified PCR pure products were sent for Illumina Hiseq sequencing (Xu et al., 2018). Sequencing data was submitted to the National Center of Biotechnology Information (NCBI) with an accession number SUB2118508.

2.4. Construction of networks

This study hypothesizes that there is a potential for acquiring consortia that are involved in AD process by generating partitioned-network modules of differentially abundant OTUs. This work constructed an association-based network, which is similar to gene co-expression approach, to identify of the "key node" of microbial consortia by revealing the non-random but strong correlations (Faust and Raes, 2012; Wu et al., 2016). The construction of correlation-based network used the data matrix of abundant OTUs (top 100) at genus level across 90 samples. The pairwise Pearson correlation index was calculated by SPSS (v. 19.0). The profile of nodes and links based on correlation matrix was identified by Cytoscape (v. 3.3.0). A random matrix theory (RMT)-based approach was also performed to capture the topological features of networks across period I-IV among three reactors (Deng et al., 2012; Deng et al., 2016). Briefly, only the OTUs detected in more than 80% samples were selected to calculate the Spearman rank correlation matrix. A series of cut-off value from 0.01 to 0.95 were applied to obtain a specific and non-random threshold value. The network topological features including average degree, average path, betweenness, clustering coefficient, density, geodesic distance, geodesic efficiency, links number, nodes number and transitivity were calculated in MENA online pipeline (http://ieg4.rccc.ou.edu/mena/).

2.5. Statistical analysis

Raw sequencing data was filtered and analyzed using the QIIME (v. 1.7.0) (Caporaso et al., 2010). OTUs were clustered at 97% similarity by searching the UPARSE (Haas et al., 2011). Less abundant OTUs (< 80% of the samples) detected in this study were filtered to minimize the impact of rare OTUs (Wu et al., 2016). Shannon index was calculated using R package. Weighted principal coordinates analysis (PcoA), principal analysis (PCA), heatmap analysis and Welch's-test were performed using the Statistical Analysis of Metagenomic Profiles (STAMP, http://kiwi.cs.dal.ca/Software/Main_Page). Differential analysis by Welch's-test inverted at 95% with *P*-value < 0.05. Relative abundance of selected OTUs was normalized to Z-value using the SPSS (v. 19.0). Dendrogram of top OTUs was clustered using the average neighbor method (UPGMA) in Cluster (v. 3.0). Venn analysis was performed using the Venny 2.1 (http://bioinfogp.cnb.csic.es/tools/venny/index.html).

3. Results and discussion

3.1. General performance of AD

This study constructed different CSTR reactors under controlled OLR and HRT conditions (Table 1). Briefly, both R1 and R2 operated with HRT = 20 day, but R1 received a constant OLR of 3 g VS L^{-1} d^{-1} as the control, whereas R2 received the OLR ranging from 4.5 to 6.7 g VS L^{-1} d^{-1} in the following 4 periods. R3 operated under the same OLR as R2 whereas with a shorter HRT = 15 day. Generally, the daily biogas production in R1 was stabilized at ca. 540 mL g^{-1} VS d^{-1} (see Supplementary data). The gradually increased OLR to 5.2 g VS L^{-1} d^{-1} (period II) in R2 and R3 led to the increased biogas production (reached 862 and 715 mL g^{-1} VS d^{-1}, respectively). Then, biogas production in R2 (335 mL g^{-1} VS d^{-1}) and R3 (321 mL g^{-1} VS d^{-1}) both decreased to lower than R1 (540 mL g^{-1} VS d^{-1}) at OLR of 6.7 g VS L^{-1} d^{-1} condition (period IV). The conversion of macromolecules of substrates (e.g. carbohydrates, proteins or lipids) into methane mainly via hydrolysis, acidogenesis and methanogenesis processes. The organic matters are hydrolyzed and further degraded by microbes to generate VFAs, such as acetic/propionic/butyric/*iso*-butyric acids. Methanogens, the sole producer of methane, have a higher affinity with acetic acid and they can't utilize other non-acetic VFAs for methane production directly (Zhong et al., 2012). In the most common one-stage AD reactors, the hydrolysis and acidogenesis steps possess a short time that pH would drop to ca. 6.5, then it recovers to a suitable range about 6.6–7.4 for methanogens due to the sufficient buffering capacity of alkalinity (ALK). It is well recognized that the VFA/ALK ratio (usually < 0.4) is a reliable indicator for the digester stability (Xu et al., 2015). Most of OLR-related researches believe that if the digesters received a high OLR (e.g. > 5 g VS d^{-1}), pH will decline to the irreversible level (such as 4.0) due to the fast rate of hydrolysis and acidogenesis steps. Finally, methane production process will decrease or even fail because methanogens are inhibited by the excessive acidification (Fitamo et al., 2017; Zhong et al., 2012). However, this study did not observe a significant pH drop (around 7.4) or VFA accumulation (< 600 mg L^{-1}) in R2 and R3 when receiving a high OLR (period IV, OLR = 6.7 g VS L^{-1} d^{-1}) (see Supplementary data). The lower biogas production at high OLR condition in this study is more likely due to the adsorption of lipids components onto sludge microaggregates or the accumulation of toxicant from food waste (such as the high salinity), which may preclude the substrates utilization by microorganisms (Zhao et al., 2016).

3.2. Diversity of AD-related microbial community

The variable region of microbial 16S rRNA gene was amplified and sequenced using Illumina Hiseq 2500 platform. A total of 5,746,922 sequences was obtained. The average number of raw reads is ca. 63,854 per sample. After de-nosing, the high-quality reads were clustered into microbial OTUs at 97% similarity. Based on the assigned OTUs across all samples from R1, R2 and R3 across the whole periods, the general distribution of microbial community composition is summarized in Table 1. At the phylum level, the shared sequences range between 46 and 85%. While at the genus level, only 25–45% of the entire community are shared, indicating the strong microbial diversity among the reactors. Most of the microbes find in these samples require further understanding to clarify their specific role in the different AD process.

To investigate how different OLR (R1 *vs*. R2) and HRT (R2 *vs*. R3) might affect the AD-related microbiome, samples from three reactors across the whole digestion periods were collected for the quantitative analysis of microbial diversity and composition. Evaluation of α-diversity (within-sample diversity index) reveals a significant difference in three reactors (Fig. 1-a). Results find that R1 has the highest Shannon diversity. When introducing a higher organic matter as co-substrate with MWS to R2 and R3, the microbial diversity both decreased. Similarly, several studies reported a reduction in microbial diversity (such as Shannon diversity) using high OLR of urban organic waste (comprising FW, grass clippings and garden waste) as co-substrates (Fitamo et al., 2017; Zhou et al., 2017). It is suggested that an increase of VFAs concentration resulted by the higher amount of lipids and proteins in organic waste will inhibit the growth of microorganisms (Fitamo et al., 2017). However, it is not accordance with this study,

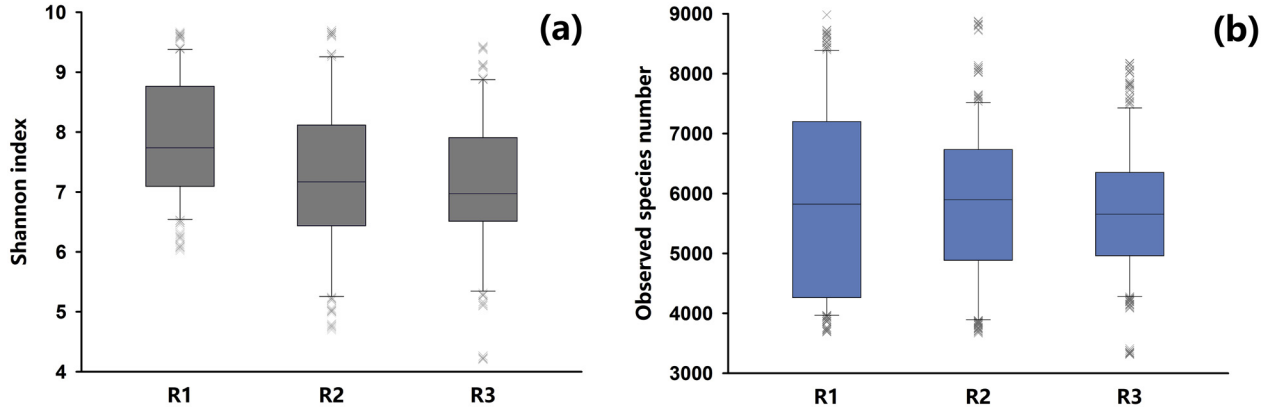

Fig. 1. With-in sample diversity (α-diversity) in three reactors along with the AD process, evaluated by (a) Shannon index and (b) Observed species number. The top and bottom of each box indicate 75% and 25% quartiles. The horizontal lines within boxes indicate median. The individual X marks indicate the outliers.

because the higher VFAs in R2 (556 mg L^{-1}) and R3 (541 mg L^{-1}) than R1 (455 mg L^{-1}) are only observed in period II temporally. Additionally, the result of Shannon index shows the microbial diversity in R3 is lower than R2. Considering the higher daily effluent volume in R3 (133 mL d^{-1}) than R2 (100 mL d^{-1}) to maintain a constant HRT value (R3 = 15 day, R2 = 20 day), thereby leading to many rare microorganisms were flushed away. Fig. 1-b confirms the R3 (5695 ± 37) has a lower number of microbes than R1 (5906 ± 35) and R2 (5832 ± 33). A low HRT is desirable to reduce the investment cost and reactor volume, but washout usually takes place when the doubling time of the microbes are shorter than the HRT. Various microbes involved in the AD process have different generation times, ranging from several hours to days (Schmidt et al., 2014). These features suggest the non-adherent microbes are less resistant to the washout due to a shorter HRT, finally leads to reactor inefficiency or inhibition of methane production in R3 (see Supplementary data).

3.3. General distribution of microbial community

Unconstrained PcoA of weighted UniFrac distances were used to evaluate the quantitative succession of microbial community structure in three reactors from period I to IV (Fig. 2). The measurement based on weighted UniFrac considers the abundance of each taxa, which is better to understand the rare members (Edwards et al., 2015). A total of 67.1% variation of microbial community composition is explained by PcoA 1 (49.3%) and PcoA 2 (17.8%), respectively. There are slight shifts in R1, because the samples are clustered closely over time when feeding with a constant OLR. The clustering pattern of microbiomes from R1 are most like each other despite 4 periods. However, for R2 and R3, the samples are clearly separated across the two axes along with different periods, indicating there are significant distinctions in the microbial community structure. The separation pattern in R2 and R3 is consistent with the OLR increasing, because the adaption of AD-related microbes is required to the introduction of new feedstocks over time. Another possible reason could be the change of sludge characters during a long-time operation. For example, the accumulation of by-products of feeding substrates, such as the salt derived from food waste, can inhibit the AD process of sludge (Zhao et al., 2016). PcoA results also describe the different HRT (R2 = 20 day *vs.* R3 = 15 day) is the second impact on the variation of microbial community, based on the similarity of distribution patterns. Because the HRT was reported to be one of the most critical conditions that affecting microbial ecology (Dareioti and Kornaros, 2014; Vasquez et al., 2017).

3.4. Changes of microbial abundance

There are remarkable variations in the specific AD-related members. Changes of the relative abundance of different microbes in three reactors across whole time are presented in Fig. 3. Considering the main OTUs, 9 phyla have greater proportions in all samples (> 1%), which are identified as the dominant members of microbial community. These dominant groups are similar with the previous studies about sludge anaerobic digesters (Fitamo et al., 2017; Rivière et al., 2009). Among them, four phyla, named *Actinobacteria*, *Bacteroidetes*, *Euryarchaeota (Archaea)*, and *Firmicutes* (alphabetical), show clear dynamics as a response to the different OLR and HRT, as marked in Fig. 3. Microorganisms classifying to phylum *Proteobacteria* (31–32%) and *Actinobacteria* (25–28%) are dominated at the beginning (day 1). *Proteobacteria* decreases to less than 10% in the following AD process among three reactors. During the AD of constant feedstocks in R1, the relative abundance of *Actinobacteria* remains predominant through the whole process, but *Actinobacteria* depletes to minor groups R2 and R3

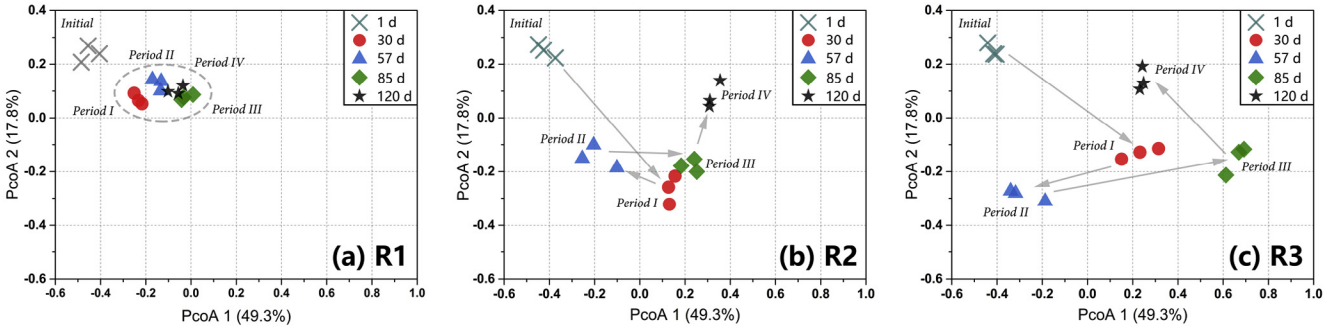

Fig. 2. Weighted principal coordinates analysis (PcoA) depicts the microbial communities are separable by OLR and HRT in R1, R2 and R3. Samples from different periods are represented by colorful symbols. The oval indicates a cluster pattern whereas the arrow indicates a succession pattern. (For interpretation of the references to colour in this figure legend, the reader is referred to the web version of this article.)

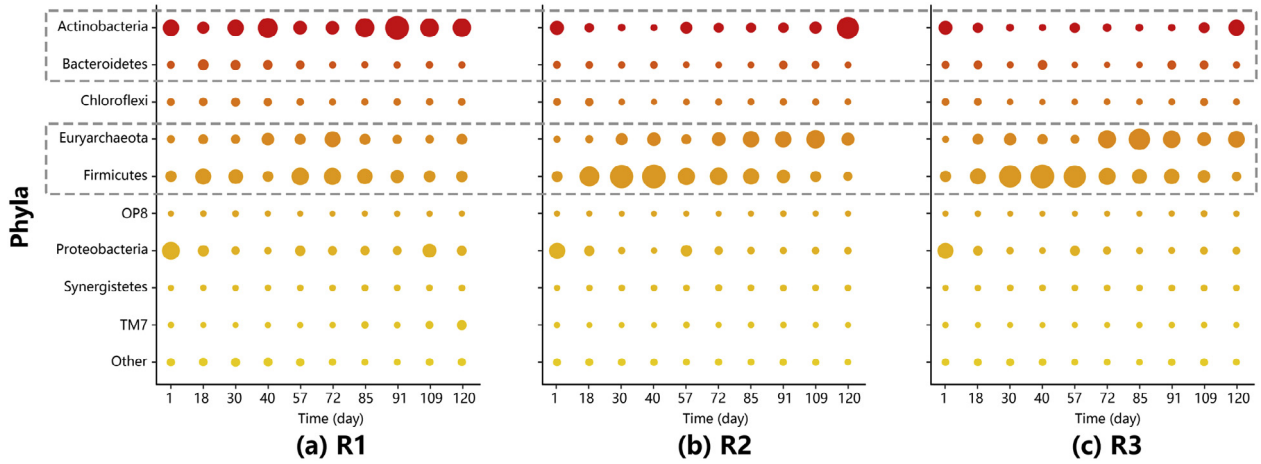

Fig. 3. Bubble diagrams of phyla relative abundance observed during the whole AD process in (a) R1, (b) R2 and (c) R3. Bubble size correlated with relative abundance of each phyla. Groups with significant difference are marked by rectangles.

when the rectors are fed with higher OLR co-substrates (except for the period IV). This result may indicate *Actinobacteria* is less favorable to the high lipids condition, which could be due to the increasing of OLR condition. Previous study also reported the phylum *Actinobacteria*, which is critical for cellulose degradation and hydrolysis, deteriorated at a shorter HRT (e.g. 10 day) condition (Wei et al., 2017). It agrees with this study, because the abundance of *Actinobacteria* is always lower in R3 (HRT = 15 day) than R2 (HRT = 20 day).

The R2 and R3 have greater proportions of the phyla *Firmicutes* (56%) and *Euryarchaeota* (49%) than R1 in period II and III. *Firmicutes* has been reported to utilize a wide range of substrates including cellulose, proteins and pectin (Fitamo et al., 2017). The predominance of *Firmicutes* in R2 and R3 can be interpreted as a higher feedstock with the OLR increasing from 4.5 to 6.7 g VS L^{-1} d^{-1}. Because previous study has reported that the phylum *Firmicutes* can degrade refractory cellulose into short-chain acids during AD process, such as acetate or propionate (Carballa et al., 2015). The higher amount of organic matters in R2 and R3 supplied more substrates for microbes, thus enriching the abundance of *Firmicutes*. Besides, *Euryarchaeota* dominates in the archaeal kingdom (> 99%), which is a well-known group participated in methane generation. From period I to IV, the relative abundance of *Euryarchaeota* increased 10-fold (from 4% to 40–50%) in R2 and R3. The enrichment of *Euryarchaeota* is according with a higher methane production in R2 and R3 (see Supplementary data).

3.5. OLR and HRT shape distinct and overlapping microbial community

The relative abundance of top OTUs belonging to family level in different reactors and different periods is shown in Fig. 4-a. To eliminate the dimension, the original data of relative abundance (sequence numbers proportion) was normalized by Z-value. Considering the 90 samples, about 95 out of 317 OTUs (at family taxonomy) are identified as dominant members. There are noteworthy overlaps in abundant OTUs among three reactors, as 38 out of 95 OTUs (40%) detected in R1 also remained relatively consistent in R2 and R3. These members show a similar distribution across the different reactors, which are denoted as the "core microbiome" in this study. Results indicate that the composition of core members consists a representation of OTUs independent of OLR or HRT conditions. The concept of "core microbiome" is defined as the smallest but functionally indispensable components of the total microbiome (Mendes et al., 2013; Qin et al., 2016). They play as generalists under different AD operation parameters and maintains the ecological stability of digesters. A recent study also observed a "core microbiome (59% of the total 16S rRNA gene sequences)" from three full-scale digesters in a wastewater treatment plant (Ran et al., 2016; Ran et al., 2017). It should be noted that nearly all the "core microbiome", as well as the α-diversity (Fig. 1-a), decreased along with the AD process, indicating a limited elasticity in maintaining stability of microbial community. Additionally, there is a set of 57 OTUs (60%) mainly belonging to the phyla *Actinobacteria*, *Firmicutes* and *Bacteroidetes* that are differentially changed in R1, R2 and R3, which are denoted as the "variable microbiome" in this study. The significant variation is according with previous result (Fig. 3), suggesting the functional redundancy in microbial communities across different operational conditions is higher than previous thought (Qin et al., 2016; Rivière et al., 2009). This indicates that only a small percentage of microbes are required to provide a series of ecological services to AD, here termed as the "core microbiome (averaged relative abundance ranging from 14%~19% in R1, R2 and R3)".

Collectively, the overall set of "core microbiome" and "variable microbiome" is defined as the pan-microbiome in this study, which is similar to the pan-genome (Tettelin et al., 2005; van Tonder et al., 2017). This study suggests that the size and composition of "core microbiome" does not vary by dataset among different collections of AD samples and their minimal variation is detectable. However, it would be more accurate to define a representative "core microbiome" if a larger number of samples and various operational parameters (e.g. ammonia concentration, temperature, substrate, or even geographical locations) are considered. Besides, as predicted in Fig. 4-a, results show that the relative abundance of several methanogenic archaea (e.g. the family *Methanosarcinaceae* and *Methanosaetaceae*) from "variable microbiome" is higher in the R2 and R3 than R1. Typically, methanogenic archaea are classified as either hydrogenotrophic or acetoclastic groups based on the substrate (molecular hydrogen or acetic acid) they consumed as the energy. In a traditional AD process, 70% methane was generated via acetoclastic groups under stable reactor conditions (Hu et al., 2015). The acetoclastic methanogens has been reported to increase when OLR was increased, because a higher amount of acetate can be fermented from the substrates, finally resulting in a higher methane yield (Razaviarani and Buchanan, 2014). *Methanosarcinaceae* and *Methanosaetaceae* are a family of the *Methanosarcinales*, which belonged to the acetoclastic methanogenic archaea. The enrichment of *Methanosarcinaceae* and *Methanosaetaceae* was accompanied by 80–95% increases in methane production in R2 (381 L) and R3 (351 L) than R1 (195 L) due to the higher OLR (Xu et al., 2015). These features can be linked to the importance of acetoclastic methanogens for a stable operation and methane generation in the AD reactors.

Venn analysis shows the characterization of core/variable microbiome using OTU counts (at genus level) from early stage and later stage (Fig. 4-b). Results reveals three reactors have discrepancy in

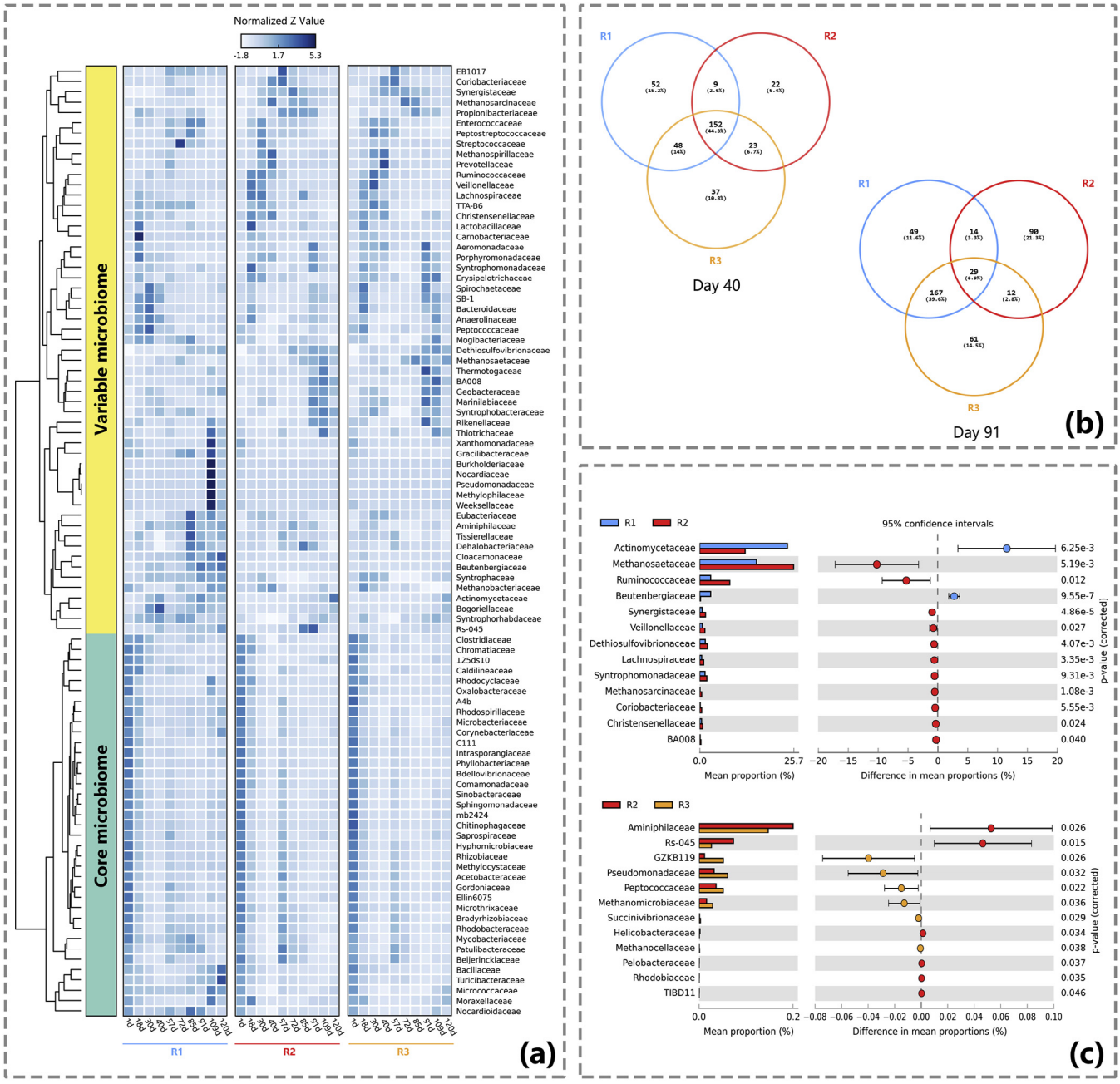

Fig. 4. Overall evaluation pan-microbiome including the overlapping ("core microbiome", marked as green) and distinct ("variable microbiome", marked as yellow) members. (a) Heatmap depicts the composition of dominant OTUs (at family level) in R1, R2 and R3. The relative abundance of each OTU is normalized by Z-value. The intensity of blue depends on the Z-value of each OTU in different samples. The sort of rows is clustered using average neighbor method (UPGMA) at the threshold of 0.75. (b) Venn analysis calculates the numbers of overlapping/distinct OTUs counts that are depleted/enriched among three reactors from day 40 to day 91. (c) Differential analysis reveals the biomarkers in OLR group (R1 *vs*. R2) and HRT group (R2 *vs*. R3), using the Welch's-test (two sided) at the confidence interval of 95% (*P*-value $<$ 0.05). Bar chart indicates the mean proportion (%) of each OTU in the reactors. (For interpretation of the references to color in this figure legend, the reader is referred to the web version of this article.)

abundant OTUs. On day 40, three reactors shared a significant overlap of abundant OTUs (152 counts), possibly representing a core microbiome for the AD process. Whereas with the prolonging of AD, only 29 OTUs (mainly *Anaerolinea*, *Brevibacillus*, *Clostridium* and *Sporosarcina*, alphabetical) can be simultaneously found among three reactors on day 91. Specifically, the number of shared OTUs between R1 and R2 significantly decreased from 161 to 43. Also, the number between R2 and R3 decreased from 175 to 41. In comparison, R2 and R3 exhibit higher enrichment ratios of distinct OTUs (from 22 to 90 and 37 to 61, respectively) than R1 (depleted from 52 to 49), indicating the OLR and HRT created the unique environment as well as R2 and R3 formed their own microbial community as a response.

The depletion level within shared OTUs varies by OLR and HRT. To explain which OTUs accounted for the operational conditions in OLR group (R1 *vs*. R2) and HRT group (R2 *vs*. R3), differential analysis was applied to reveal the significant variation (Welch's-test inverted at 95%, *P*-value $<$ 0.05) between the abundant OTUs (at family level) (Fig. 4-c). The biomarkers are mainly identified as *Actinomycetaceae*, *Methanosaetaceae*, *Ruminococcaceae* in OLR group. The mean proportion of *Methanosaetaceae* and *Ruminococcaceae* was two-times abundant in R2 than R1. *Ruminococcaceae* is identified as a representative member within the phylum *Firmicutes* in anaerobic condition, which can degrade

a wide range of substrates (e.g. cellulose and proteins) (Fitamo et al., 2017). The enrichment of *Ruminococcaceae* in R2 confirms the higher amount of proteins and fats in the increasing OLR condition. Besides, the traditional AD process mainly generated methane via the acetoclastic methanogen pathway (De et al., 2012) under low acetic acid condition. *Methanosaetaceae* is profiled as a aceticlastic species that has a higher affinity for acetic acid than other common methanogenic archaea, such as the order *Methanomicrobiales* and *Methanosarcinaceae* (Yuan et al., 2014). The higher abundance of *Methanosaetaceae* can be attributed to the higher acetic acid that degraded from higher organic matters in R2, resulting a higher methane production with the increasing OLR (see Supplementary data). Moreover, 12 OTUs are found to be significantly affected by HRT condition. The biomarkers mainly consisting the family *GZKB119*, *Pseudomonadaceae*, *Peptococcaceae* and *Methanomicrobiaceae* are enriched in R3. *Methanomicrobiaceae* are profiled as typical methanogens members that using H_2/CO_2 and formate as substrates. It is reported that stressful conditions (e.g. decreased HRTs in R3, or sudden loading shocks, temperature variations, ammonium accumulation, etc.) can promote the abundance of *Methanomicrobiaceae* with a shift from aceticlastic methanogens (e.g. *Methanosaetaceae*) to syntrophic acetate oxidation followed by hydrogenotrophic methanogens (e.g. *Methanomicrobiaceae*) (Werner et al., 2014). A similar study also confirmed the further reduction of HRT to 1.5 days resulted in the predominance of hydrogenotrophic methanogens (Schmidt et al., 2014). Not surprisingly, the HRT caused a less effect on microorganisms than OLR. Because the mean abundance profile of biomarkers in HRT group ranged from 0 to 0.2%, which is much rare than OLR group (ranging from 0 to 25.7%). The discrepancy of effect size caused by OLR and HRT agrees with previous analysis (Figs. 1–4-b), indicating OLR variation shaped a more diverse microbiome in R2 than R3.

3.6. Identification of the networks of AD-related microbiomes

To explore the co-occurrence interactions within partner-groups, this study applied molecular ecological network to characterize AD-related microbiomes across time-series data under different OLR and HRT (Fig. 5). Because the most advantage of AD technology is the generation of methane, this work mainly focused on the identification of consortia involved in methane generation, including 3 fermentative bacteria (the phyla *Actinobacteria*, *Bacteroidetes* and *Firmicutes*) and 1 methanogenic archaea (the phylum *Euryarchaeota*). Considering the advantages of calculation procedure and noise tolerance of raw data, the correlation-based network was selected. Briefly, the two-sides Pearson test determined the pairwise correlations between abundant OTUs from the OLR group (R1 *vs*. R2) and HRT group (R2 *vs*. R3). Then, the significantly correlated components (P-value < 0.05, $r > 0.8$) were selected to construct the molecular ecological networks. Because different microorganisms share a strong syntrophic relationship, so that no partner can conduct a metabolic task exclusively. Network correlations suggest the co-colonization and niche overlap within the microbiomes (Faust and Raes, 2012). The positive correlation usually indicates a similar behavior of microbial adaptation (Edwards et al., 2015). In total, 12 and 6 modules were identified in OLR-network and HRT-network, respectively. The main modules could be interpreted as different function components within microbial community (Deng et al., 2016). The degree of modularity in OLR-network is higher than the HRT-network, suggesting the further subdivision of AD-related microbiomes into function components (Wu et al., 2016). Accordingly, microbial communities prefer to cluster together within each module and their distribution become less even over time, resulting a higher bio-diversity in the reactor (R2 > R3, Fig. 1). In fact, bio-diversity is important to maintain the stability of digesters when facing the shock of operation variables, such pH, OLR or temperature (Wittebolle et al., 2009). Because the diverse members are more likely to vary with each other asynchronously, providing chances to maintain the stability of digesters (Kundu et al., 2017). Thus, microbial communities rely less on the dominant groups if they are highly diverse and digesters will be less distracted by the operation variables (Wittebolle et al., 2009). In this study, the higher biogas production was confirmed by the higher modularity and Shannon diversity in R2 than R3.

In the generated nodes, OLR-network and HRT-network have a similar targeted phyla nodes number (42% *vs*. 44%). The rest nodes mainly belong to the phyla *Chloroflexi*, *Proteobacteria* and *Synergistetes*. Such commonly detectable nodes/links suggest there is a flexible group behaves as super-generalists in different AD conditions (Wu et al., 2016). In addition, the phylum *Firmicutes* was identified as the top connection node in OLR-network (14/63) and HRT-network (15/59). Previous studies suggested that the hub OTUs identified by network method are significant in maintaining the stability or efficiency of AD reactors (Wu et al., 2016). This study found that the dynamic of *Firmicutes* was positively correlated with biogas production ($r > 0.62$, P-value < 0.05). This confirmed with the fact that *Firmicutes* is known as a fermentative member for the degradation of organic substrates, indicating their critical roles in the acetogenic metabolism with a final product of acetate (Fitamo et al., 2017; Rincón et al., 2008). Besides, results also indicate OLR and HRT conditions have shaped two AD-microbiomes due to the significantly different interactions from two networks. In a survey of granular sludge-based reactors, Kundu et al. also observed the organic and hydraulic shocks resulted in different level of tolerance of microbial communities (Kundu et al., 2017). In the pair-wise links, OLR-network (126 links) an HRT- network (151 links) only shares 12 links (4.5%), such as *Methanosphaera-Azospira* and *Pseudomonas-Methanosphaera*. The rare links number shared between OLR and HRT networks might due to the temporary interactions or ecological drift of microbial communities (Edwards et al., 2015). Additionally, network analysis provides an overview that the less abundant OTUs (light blue nodes in Fig. 5) also significantly contributes to interaction of AD-related microbiomes, such as the genus *Methanospirillum*, *Methanosphaera*, *Bacillus* and *Geobacter*. Result shows that methane production process is affected not only by dominant microorganisms, but also by rare members. Qin et al. as well as reviewed the less abundant taxa should not be overlooked because they are crucial in maintaining the community functions (Qin et al., 2016). Further work is required to better understand the important roles of these rare microbes (Xu et al., 2017).

3.7. Correlation of network topological characteristics and AD parameters

Relationships among network topological features (including average degree, average path, betweenness, clustering coefficient, density, geodesic distance, geodesic efficiency, links number, nodes number and transitivity), microbial community features (Shannon diversity, abundance of *Firmicutes*, *Actinobacteria*, *Euryarchaeota*, *Bacteroidetes*, *Methanomethylovorans* and *Methanomassilicoccus*) and AD variables were further analyzed by PCA and Pearson correlation methods (Fig. 6). In order to capture the network topological features, this study constructed 12 networks (N1-12) based on time-lagging RMT approach using 90 samples due to the different periods. RMT threshold values ranges from 0.31 to 0.89. Details of network characteristics were summarized in Supplementary data. Biogas production, VFA/ALK ratio and pH were selected as AD variables in this study because these critical parameters correlated with methane yield and reactor stability, which are the first thing people paid attention to (Xu et al., 2015). A total of 73.3% variation can be explained by two components (50.8% for PC 1 and 22.5% for PC 2, see Supplementary data). Results show that VFA/ALK ratio was strongly correlated with transitivity ($r > 0.68$, P-value < 0.05) and clustering coefficient ($r > 0.61$, P-value < 0.05). pH was mainly correlated with links number ($r < -0.81$, P-value < 0.01). But biogas production shows a few correlations with nodes number, links number and clustering coefficient ($r < 0.38$). Moreover, the network topological features also correlated with the dynamics of

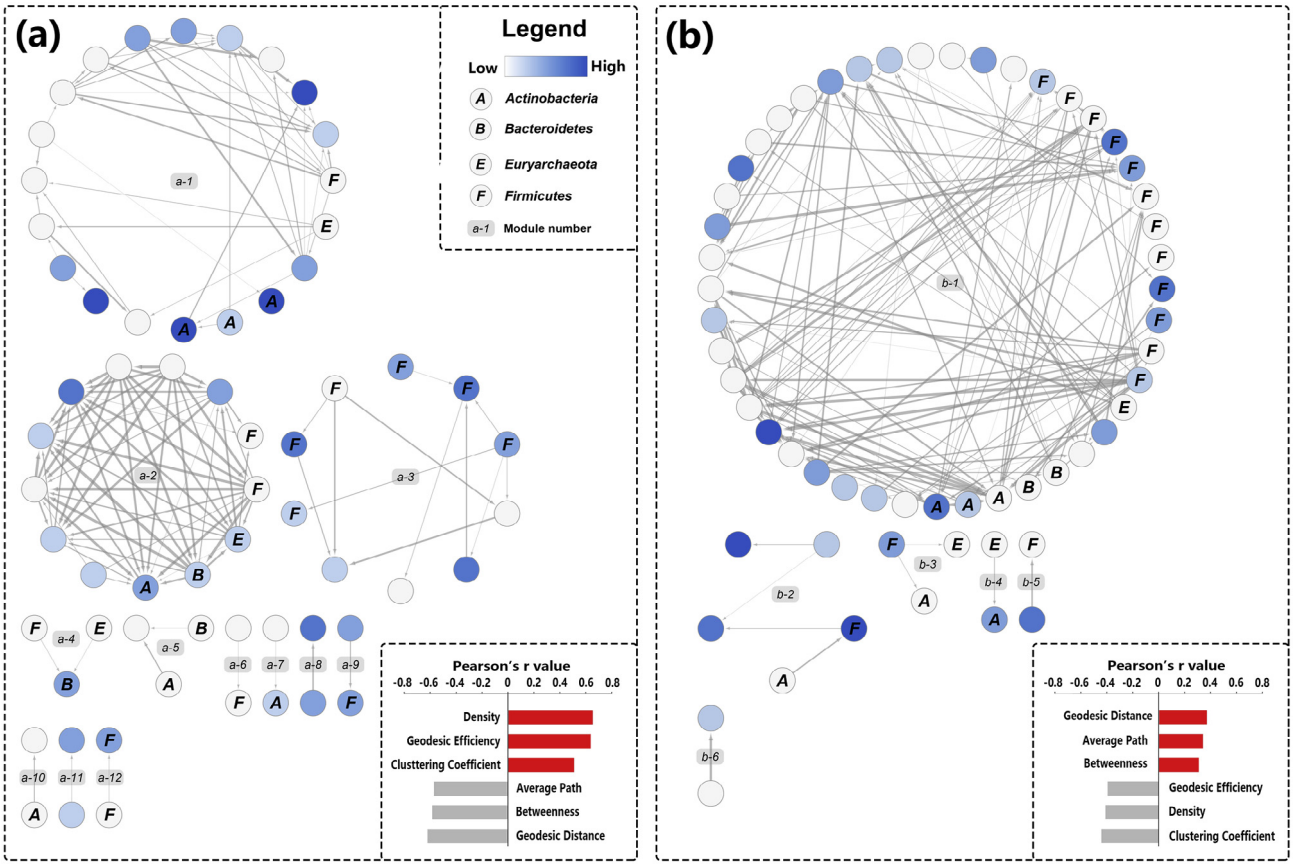

Fig. 5. Molecular ecological networks reveal the OTUs modules associated with methane generation taxonomies (*Actinobacteria*, *Bacteroidetes*, *Firmicutes* and *Euryarchaeota*) are affected by: (a) OLR and (b) HRT. Each node represents 1 OTUs belonged to 4 phyla that mainly involved in methane generation. Color intension (from light to dark) of node represents the mean abundance (from low to high) profile of selected OTU. Nodes are connected by the pairwise interactions (links). Weight of link indicates a strong Pearson correlation ($r > 0.8$, P-value < 0.01) that shared between OTUs.

AD-related members. For example, the geodesic distance, betweenness and average path were positively correlated with *Methanomethylovorans* ($r > 0.64$, P-value < 0.05). While average degree, clustering coefficient, geodesic efficiency and density were negatively correlated with *Actinobacteria* and *Methanomethylovorans* ($-0.80 < r < -0.51$, P-value < 0.05). Although *Methanomethylovorans* is suggested as important member in the microbial communities' network, however, *Methanomethylovorans* is profiles as an uncultured strain and comprised less than 0.04% in all samples (Gagliano et al., 2017). The specific function of *Methanomethylovorans* in anaerobic digestion remains to be characterized.

Overall, this work has proved OLR and HRT would exert different impacts on microbial ecology and disposal capacity of the digesters, which may further affect the investment decisions on AD facilities. The network of modules revealed the known taxonomies to be involved in methane production, as well as many additional unknown OTUs. Although many of the detectable OTUs from network modules have limited available information in terms of taxonomic or function, results still show that an OTU correlation-based network approach helps to recapitulate microbial associations from empirical data. Although HTS broadened the understanding to the culture-independent microbes from a complex system, it is essential to evaluate how the potential error can impact the results of biological relevance. Because such "comparative metagenomics" largely relies on the reliable annotation of sequencing reads against the reference databases. It also should be noted that the statistical significance is usually used to filter uninteresting statistical properties with some criterions for biological relevance. Thus, the observed statistical significance of enrichment or depletion in this study requires more approaches to validate their biologically relevant (e.g. the differentiation that comes from those truly taxonomic or ecological phenomenon). Further larger-scale studies on the identified keystone species would be informative to enhance AD performance and efficiency, such as identifying the novel microbial associations, bioaugmenting the key members, establishing a mathematical modeling based on structure–function, or developing proper tools to interpret microbiological data for routine monitoring by the engineers (Briones and Raskin, 2003; Carballa et al., 2015; Ferguson et al., 2016; Ferguson et al., 2014; Kundu et al., 2017; Tale et al., 2015). With the purpose of increasing biogas production, it is possible to use the information regarding the "core microbiome" to design a robust co-culture system of synthetic microbial comminutes, which can bridge the gap between basic research and practical application.

4. Conclusions

This study presents new approaches toward understanding the evolution of AD-related microbiomes and the operational parameters that influence them. Structures of the phyla *Actinobacteria*, *Bacteroidetes*, *Euryarchaeota*, and *Firmicutes* were largely affected by OLR and HRT. AD-related microbiomes are more homogeneous than previous thought, because a set of 40% core OTUs are similar in the digesters irrespective of the OLR or HRT. The most connected node of *Firmicutes* are positively correlated with biogas production based on network topological features. Priority regulation of keystone members within microbial networks will encourage future developments of AD design to increase methane production or operation stability.

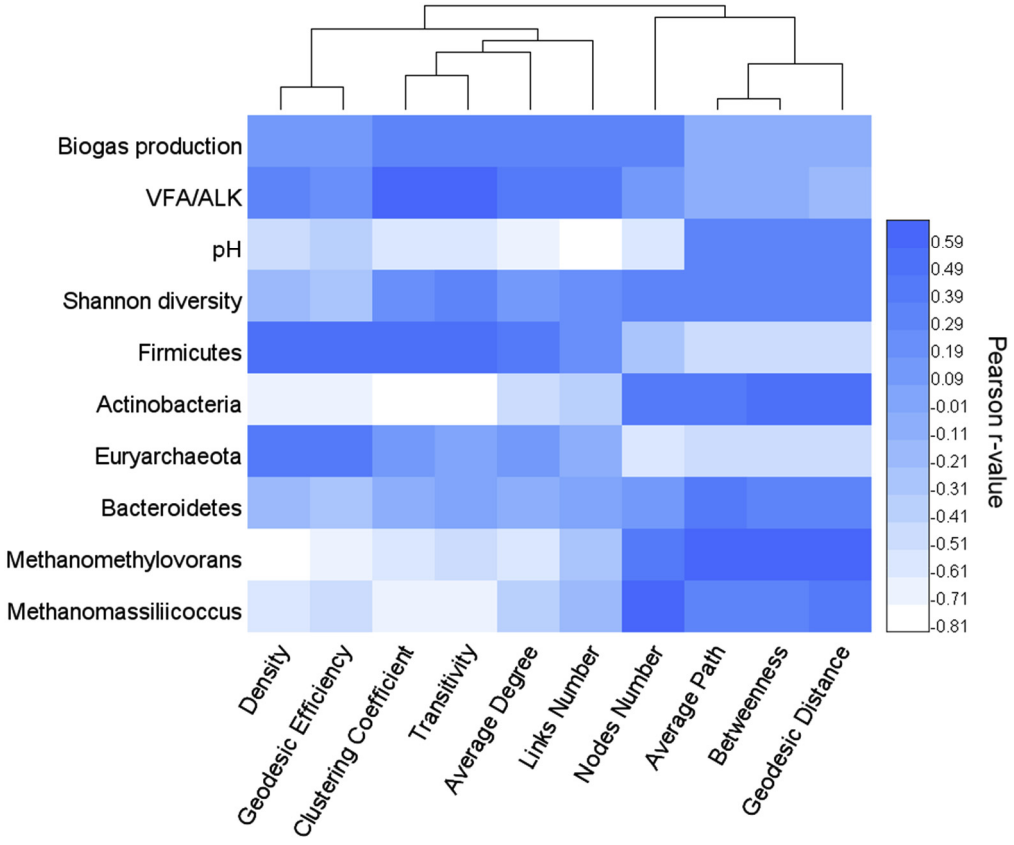

Fig. 6. Correlations among network topological features (x-axis), microbial community features and anaerobic digestion variables. The color intensive represents a Pearson correlation value (P-value < 0.05).

Acknowledgments

The study was financially supported by the Key Research and Development Program of Hunan Province (2017SK2242), China and National Natural Science Foundation of China (51578223 and 51521006).

Appendix A. Supplementary data

Supplementary data associated with this article can be found, in the online version, at https://doi.org/10.1016/j.biortech.2018.04.083.

References

Anantharaman, K., Brown, C.T., Hug, L.A., Sharon, I., Castelle, C.J., Probst, A.J., Thomas, B.C., Singh, A., Wilkins, M.J., Karaoz, U., Brodie, E.L., Williams, K.H., Hubbard, S.S., Banfield, J.F., 2016. Thousands of microbial genomes shed light on interconnected biogeochemical processes in an aquifer system. Nat. Commun. 7, 13219.

Briones, A., Raskin, L., 2003. Diversity and dynamics of microbial communities in engineered environments and their implications for process stability. Curr. Opin. Biotechnol. 14 (3), 270–276.

Caporaso, J.G., Kuczynski, J., Stombaugh, J., Bittinger, K., Bushman, F.D., Costello, E.K., et al., 2010. QIIME allows analysis of high-throughput community sequencing data. Nat. Method 7, 335–336.

Carballa, M., Regueiro, L., Lema, J.M., 2015. Microbial management of anaerobic digestion: exploiting the microbiome-functionality nexus. Curr. Opin. Biotechnol. 33, 103–111.

Dareioti, M.A., Kornaros, M., 2014. Effect of hydraulic retention time (HRT) on the anaerobic co-digestion of agro-industrial wastes in a two-stage CSTR system. Bioresour. Technol. 167 (3), 407–415.

De, V.J., Hennebel, T., Boon, N., Verstraete, W., 2012. Methanosarcina: the rediscovered methanogen for heavy duty biomethanation. Bioresour. Technol. 112 (5), 1–9.

De Vrieze, J., Pinto, A.J., Sloan, W.T., Ijaz, U.Z., 2018. The active microbial community more accurately reflects the anaerobic digestion process: 16S rRNA (gene) sequencing as a predictive tool. Microbiome 6 (1), 63.

De Vrieze, J., Raport, L., Roume, H., Vilchez-Vargas, R., Jáuregui, R., Pieper, D.H., Boon, N., 2016. The full-scale anaerobic digestion microbiome is represented by specific marker populations. Water Res. 104, 101–110.

Deng, Y., Jiang, Y.H., Yang, Y., He, Z., Luo, F., Zhou, J., 2012. Molecular ecological network analyses. BMC Bioinf. 13 (1), 113.

Deng, Y., Zhang, P., Qin, Y., Tu, Q., Yang, Y., He, Z., Schadt, C.W., Zhou, J., 2016. Network succession reveals the importance of competition in response to emulsified vegetable oil amendment for uranium bioremediation. Environ. Microbiol. 18 (1), 205–218.

Edwards, J., Johnson, C., Santosmedellín, C., Lurie, E., Podishetty, N.K., Bhatnagar, S., Eisen, J.A., Sundaresan, V., 2015. Structure, variation, and assembly of the root-associated microbiomes of rice. PNAS 112 (8), E911.

Faust, K., Raes, J., 2012. Microbial interactions: from networks to models. Nat. Rev. Microbiol. 10 (8), 538.

Ferguson, R.M.W., Coulon, F., Villa, R., 2016. Organic loading rate: a promising microbial management tool in anaerobic digestion. Water Res. 100, 348–356.

Ferguson, R.M.W., Villa, R., Coulon, F.D.R., 2014. Bioengineering options and strategies for the optimization of anaerobic digestion processes. Environ. Technol. Rev. 3 (1), 1–14.

Fitamo, T., Treu, L., Boldrin, A., Sartori, C., Angelidaki, I., Scheutz, C., 2017. Microbial population dynamics in urban organic waste anaerobic co-digestion with mixed sludge during a change in feedstock composition and different hydraulic retention times. Water Res. 118, 261–271.

Gagliano, M.C., Ismail, S.B., Stams, A.J.M., Plugge, C.M., Temmink, H., Van Lier, J.B., 2017. Biofilm formation and granule properties in anaerobic digestion at high salinity. Water Res. 121, 61–71.

Gou, C., Yang, Z., Huang, J., Wang, H., Xu, H., Wang, L., 2014. Effects of temperature and organic loading rate on the performance and microbial community of anaerobic co-digestion of waste activated sludge and food waste. Chemosphere 105 (3), 146–151.

Haas, B.J., Gevers, D., Earl, A.M., Feldgarden, M., Ward, D.V., Giannoukos, G., Ciulla, D., Tabbaa, D., Highlander, S.K., Sodergren, E., 2011. Chimeric 16S rRNA sequence formation and detection in Sanger and 454-pyrosequenced PCR amplicons. Genome Res. 21 (3), 494.

He, H., Liu, Y., Wang, X., Huang, Z., Xu, C., Yang, T., Zhang, Z., Wang, L., Ma, J., 2018. Effects of newly prepared alkaline ferrate on sludge disintegration and methane production: reaction mechanism and model simulation. Chem. Eng. J. 343, 520–529.

Hu, Y., Hao, X., Zhao, D., Fu, K., 2015. Enhancing the CH4 yield of anaerobic digestion via endogenous CO2 fixation by exogenous H2. Chemosphere 140, 34–39.

Kuczynski, J., Stombaugh, J., Walters, W.A., González, A., Caporaso, J.G., Knight, R., 2011. Using QIIME to Analyze 16S rRNA Gene Sequences from Microbial Communities. John Wiley & Sons Inc.

Kumar, G., Sivagurunathan, P., Park, J.H., Sang, H.K., 2016. Anaerobic digestion of food waste to methane at various organic loading rates (OLRs) and hydraulic retention times (HRTs). Environ. Eng. Res. 21.

Kundu, K., Sharma, S., Sreekrishnan, T.R., 2017. Influence of process parameters on anaerobic digestion microbiome in bioenergy production: towards an improved understanding. Bioenergy Res. 10 (1), 288–303.
Lynch, Neufeld, 2015. Ecology and exploration of the rare biosphere. Nat. Rev. Microbiol. 13 (4), 217.
Ma, B., Wang, H., Dsouza, M., Lou, J., He, Y., Dai, Z., Brookes, P.C., Xu, J., Gilbert, J.A., 2016. Geographic patterns of co-occurrence network topological features for soil microbiota at continental scale in eastern China. ISME J. 10 (8), 1891.
Mendes, R., Garbeva, P., Raaijmakers, J.M., 2013. The rhizosphere microbiome: significance of plant beneficial, plant pathogenic, and human pathogenic microorganisms. FEMS Microbiol. Rev. 37 (5), 634–663.
Qin, Y., Druzhinina, I.S., Pan, X., Yuan, Z., 2016. Microbially mediated plant salt tolerance and microbiome-based solutions for saline agriculture. Biotechnol. Adv. 34 (7), 1245–1259.
Ran, M., Narihiro, T., Nobu, M.K., Kuroda, K., Liu, W.T., 2016. Evaluating digestion efficiency in full-scale anaerobic digesters by identifying active microbial populations through the lens of microbial activity. Sci. Rep. 6, 34090.
Ran, M., Nobu, M.K., Narihiro, T., Kuroda, K., Sierra, J.M., Wu, Z., Lin, Y., Lee, P.K.H., Lee, P.H., Lier, J.B.V., 2017. Operation-driven heterogeneity and overlooked feed-associated populations in global anaerobic digester microbiome. Water Res. 7 (1), 77–84.
Razaviarani, V., Buchanan, I.D., 2014. Reactor performance and microbial community dynamics during anaerobic co-digestion of municipal wastewater sludge with restaurant grease waste at steady state and overloading stages. Bioresour. Technol. 172, 232–240.
Rincón, B., Borja, R., González, J.M., Portillo, M.C., Sáiz-Jiménez, C., 2008. Influence of organic loading rate and hydraulic retention time on the performance, stability and microbial communities of one-stage anaerobic digestion of two-phase olive mill solid residue. Biochem. Eng. J. 40 (2), 253–261.
Rivière, D., Desvignes, V., Pelletier, E., Chaussonnerie, S., Guermazi, S., Weissenbach, J., Li, T., Camacho, P., Sghir, A., 2009. Towards the definition of a core of microorganisms involved in anaerobic digestion of sludge. ISME J. 3 (6), 700–714.
Schmidt, T., Ziganshin, A.M., Nikolausz, M., Scholwin, F., Nelles, M., Kleinsteuber, S., Pröter, J., 2014. Effects of the reduction of the hydraulic retention time to 1.5 days at constant organic loading in CSTR, ASBR, and fixed-bed reactors - performance and methanogenic community composition. Biomass Bioenergy 69 (122), 241–248.
Tale, V.P., Maki, J.S., Zitomer, D.H., 2015. Bioaugmentation of overloaded anaerobic digesters restores function and archaeal community. Water Res. 70, 138–147.
Tettelin, H., Masignani, V., Cieslewicz, M.J., Donati, C., Medini, D., Ward, N.L., Angiuoli, S.V., Crabtree, J., Jones, A.L., Durkin, A.S., 2005. Genome analysis of multiple pathogenic isolates of Streptococcus agalactiae: implications for the microbial "pan-genome". PNAS 102 (39), 13950–13955.
van Tonder, A.J., Bray, J.E., Jolley, K.A., Quirk, S.J., Haraldsson, G., Maiden, M.C.J., Bentley, S.D., Haraldsson, A., Erlendsdottir, H., Kristinsson, K.G., Brueggemann, A.B., 2017. Heterogeneity among estimates of the core genome and pan-genome in different pneumococcal populations. bioRxiv.
Vasquez, Y., Escobar, M.C., Saenz, J.S., Quicenovallejo, M.F., Neculita, C.M., Arbeli, Z., Roldan, F., 2017. Effect of hydraulic retention time on microbial community in biochemical passive reactors during treatment of acid mine drainage. Bioresour. Technol. 247, 624–632.
Wei, L., An, X., Wang, S., Xue, C., Jiang, J., Zhao, Q., Kabutey, F.T., Wang, K., 2017. Effect of hydraulic retention time on deterioration/restarting of sludge anaerobic digestion: extracellular polymeric substances and microbial response. Bioresour. Technol. 244, 261–269.
Werner, J.J., Garcia, M.L., Perkins, S.D., Yarasheski, K.E., Smith, S.R., Muegge, B.D., Stadermann, F.J., Derito, C.M., Floss, C., Madsen, E.L., 2014. Microbial community dynamics and stability during an ammonia-induced shift to syntrophic acetate oxidation. Appl. Environ. Microbiol. 80 (11), 3375–3383.
Wittebolle, L., Marzorati, M., Clement, L., Balloi, A., Daffonchio, D., Heylen, K., De, V.P., Verstraete, W., Boon, N., 2009. Initial community evenness favours functionality under selective stress. Nature 458 (7238), 623–626.
Wu, L., Yang, Y., Chen, S., Zhao, M., Zhu, Z., Yang, S., Qu, Y., Ma, Q., He, Z., Zhou, J., He, Q., 2016. Long-term successional dynamics of microbial association networks in anaerobic digestion processes. Water Res. 104, 1–10.
Xu, R., Yang, Z.H., Chen, T., Zhao, L., Huang, J., Xu, H., Song, P., Li, M., 2015. Anaerobic co-digestion of municipal wastewater sludge with food waste under different fat, oil, grease contents: study on reactor performance and extracellular polymeric substances. RSC Adv. 5, 103547–103556.
Xu, R., Yang, Z.H., Wang, Q.P., Bai, Y., Liu, J.B., Zheng, Y., Zhang, Y.R., Xiong, W.P., Ahmad, K., Fan, C.Z., 2018. Rapid startup of thermophilic anaerobic digester to remove tetracycline and sulfonamides resistance genes from sewage sludge. Sci. Total Environ. 612 (112), 788–798.
Xu, R., Yang, Z.H., Zheng, Y., Zhang, H.B., Liu, J.B., Xiong, W.P., Zhang, Y.R., Ahmad, K., 2017. Depth-resolved microbial community analyses in the anaerobic co-digester of dewatered sewage sludge with food waste. Bioresour. Technol. 244, 824–835.
Yuan, X., Wen, B., Ma, X., Zhu, W., Wang, X., Chen, S., Cui, Z., 2014. Enhancing the anaerobic digestion of lignocellulose of municipal solid waste using a microbial pretreatment method. Bioresour. Technol. 154 (1), 1.
Zhao, J., Zhang, C., Wang, D., Li, X., An, H., Xie, T., Chen, F., Xu, Q.X., Sun, Y., Zeng, G., 2016. Revealing the underlying mechanisms of how sodium chloride affects short-chain fatty acid production from the co-fermentation of waste activated sludge and food waste. ACS Sustain. Chem. Eng. 4 (9).
Zhong, W.Z., Zhang, Z.Z., Luo, Y.J., Qiao, W., Xiao, M., Zhang, M., 2012. Biogas productivity by co-digesting Taihu blue algae with corn straw as an external carbon source. Bioresour. Technol. 114 (3), 281–286.
Zhou, J., Yang, J., Yu, Q., Yong, X., Xie, X., Zhang, L., Wei, P., Jia, H., 2017. Different organic loading rates on the biogas production during the anaerobic digestion of rice straw: a pilot study. Bioresour. Technol. 244, 865–871.
Ziganshin, A.M., Schmidt, T., Lv, Z., Liebetrau, J., Richnow, H.H., Kleinsteuber, S., Nikolausz, M., 2016. Reduction of the hydraulic retention time at constant high organic loading rate to reach the microbial limits of anaerobic digestion in various reactor systems. Bioresour. Technol. 217, 62–71.